Electrochimica Acta 508 (2024) 145280

Contents lists available at ScienceDirect

Electrochimica Acta

journal homepage: www.journals.elsevier.com/electrochimica-acta

An assessment of electroneutrality implementations for accurate electrochemical ion transport models

Benjamin Janotta [a,*], Maximilian Schalenbach [a,*], Hermann Tempel [a], Rüdiger-A. Eichel [a,b]

[a] Fundamental Electrochemistry (IET-1), Institute of Energy Technologies, Forschungszentrum Jülich, Wilhelm-Johnen-Straße, 52425 Jülich, Germany
[b] Institute of Physical Chemistry, RWTH Aachen University, 52062 Aachen, Germany

ARTICLE INFO

Keywords:
Electroneutrality
Electrolytes
Ion transport
Simulation
Nernst-Planck

ABSTRACT

During the diffusion and migration of ions in electrolytes, the electrodynamic ion-ion interactions prevent charge separation despite different ionic mobilities, ultimately enforcing electroneutrality in the bulk electrolyte. To model ion transport accurately, a method to enforce electroneutrality must be implemented. In this study, four strategies to implement electroneutrality are discussed and evaluated. The ion distributions that result from a transport model with the different electroneutrality implementations are calculated, considering various electrolytes and sets of electrochemical parameters. The meaningfulness and applicability of each implementation are assessed through spatial charge accumulations, transference numbers, and experimental data from the literature. Combining the electrochemical ion transport models with the electroneutrality constraint for all ions is shown to result in an overdetermined system of equations if the driving forces are calculated under neglection of diffusion potentials. The often-reported model simplification of using the electroneutrality constraint to resolve the transport of one specific species explicitly results in non-physically correct mass transport. A practical approach to precisely describe the measured physicochemical ion movements is obtained by equilibrating spatial charges with the ion conduction for every time step in the ion transport model, which is reasonably applicable to multi-ion systems in three-dimensional frameworks. This comprehensive assessment aims to guide readers in selecting an appropriate electroneutrality implementation framework for ion transport models.

1. Introduction

Inside an electrolyte, Coulomb forces between ions enforce macroscopic electroneutrality [1,2], as spatial charge accumulations in the bulk are directly equilibrated by electric field-driven ion movement [2,3]. However, at the electrodes, the electrolyte compensates for surface charges by forming non-electroneutral double layers. In electrostatic equilibrium (no current), the double layers shield the potential differences between electrodes, preventing a macroscopic electric field within the bulk electrolyte [4]. A macroscopic electric field inside the bulk electrolyte leads to an ion current, yet, the bulk solution remains electroneutral [5]. To portray the physics of electrolytic solution in ion transport models accurately, employing the electroneutrality constraint displays a major component [1].

In electrochemical cells with liquid electrolytes, the ion transport leads to locally different ion concentrations [6–8], conductivities [9], and electric fields [7,10–12], which ultimately affect the limited currents [7,9], reaction rates [13], and reactor efficiencies [14]. Ion transport models describe the time-evolution of ion movement in electrochemical cells, making local ion concentrations predictable [6]. Hence, these models are powerful tools to optimize process parameters [11,15], and product compositions [13]. As reviewed by Rivera et al. [16]., precise transport models and accurate parameterization of the physicochemical electrolyte properties are required to accurately resemble the ion transport in real electrochemical cells. Typically, four types of equations are necessary to properly calculate ion transport [1,17,18]: (i) a mass balance in the form of the mass conservation equation; (ii) the relation between fluxes of ionic species and the current (Faraday's law); (iii) a model for the (ionic) fluxes; (iv) the electroneutrality constraint. The first two relations are inevitable and unambiguously necessary for every ion transport model, while the latter two can be evaluated by different approaches.

The validity and applicability of flux models in electrochemical systems is discussed ever since the development of the Nernst-Planck theory [19–21] for ions at infinite dilution in 1888. The Nernst-Planck theory describes the ion fluxes as superposition of the contributions of

* Corresponding authors.
E-mail addresses: b.janotta@fz-juelich.de (B. Janotta), m.schalenbach@fz-juelich.de (M. Schalenbach).

https://doi.org/10.1016/j.electacta.2024.145280
Received 8 August 2024; Received in revised form 17 October 2024; Accepted 22 October 2024
Available online 23 October 2024

diffusion and migration, neglecting ion-ion interactions [2,18]. In 1931, Onsager [22] further developed ion transport models by linking the flux (or velocity) of a species linearly to the gradient in electrochemical potential $\nabla\mu_k$ of that species with respect to all species in solution. Thus, he extended the previously developed Maxwell-Stefan [23,24] matrices that describe the interaction of the diffusion in multi-component gases. Newman et al. [1,25] proposed the concentrated solution theory which is similar to Onsager's model, but features an easier parameterization of the electrolyte properties regarding the temperature and concentration dependence. Models based on the concentrated solution theory estimate the interaction of different components in electrolytes, yet, the parameterization of such interactions lacks available data (Newman et al. [1], p. 261f.). Nevertheless, these models are widely used in recent studies and now commonly regarded as standard to describe ion transport [26,27]. The advantages and disadvantages of ion transport models are compared in several studies [17,28–31], highlighting the importance of employed parametrizations and experimental validations.

Table 1 summarizes exemplary recent studies on ion transport in electrolytes and their model characteristics. A comparison of these and other studies revealed four applied methods (denoted by M1 to M4, described in detail in the methods section) to incorporate the electroneutrality constraint in ion transport models. León et al. [32] reported a comparable table with a focus on transport equations for electrodialysis simulations. These methodologies describe different physicochemical meanings and require evaluation and comparison to real experimental data. For a precise modelling of experimental data, the concentration dependence of physicochemical properties such as conductivities, diffusion coefficients, and transference numbers must be considered [7], which however was neglected by most studies found.

Here, a hands-on comparison of the four different methods to implement the electroneutrality constraint in ion transport models is presented. Spatial charge distributions in various electrochemical setups are modelled with each of these methods, showing their physicochemical plausibility. Moreover, experimental data from the literature are described with the different methods to implement the electroneutrality constraint, aiming to highlight precise modelling of real ion transport. In an assertation matrix, the advantages, and disadvantages of the different methods for the electroneutrality constraint are compared. In this study, the electrochemical transport is discussed in one dimension solely focussing on diffusion and electric field driven transport. More dimensions and the convection-driven transport can be added to the presented models, yet these complicate the mathematical description.

2. Methods

2.1. Ion transport models

Electrochemical ion transport is mathematically represented by a system of non-linear partial differential equations that is constrained by the electroneutrality condition. For each species, the mass conservation equation (Eq. (1a)) and an equation for the flux as a function of the driving forces predict the spatiotemporal concentration. In this work, a one-dimensional framework is applied, and the Nernst-Planck equation (Eq. (1b)) is used to describe the flux of each species. The electroneutrality constraint (Eq. (1c)) represents a charge balance that enforces divergent-free charge transport. Eq. (1a) - 1c must be solved with respect to each other

$$\dot{c_k} = -N_k' \qquad \forall k \tag{1a}$$

$$N_k = -D_k c_k' - \frac{z_k \lambda_k}{|z_k| F} c_k \Phi' \quad \forall k \tag{1b}$$

$$0 = \sum_j z_j \, c_j, \tag{1c}$$

where c denotes the concentration of ion type k, N the flux, D the diffusion coefficient, z the valence, λ the ionic molar conductance, F Faraday's constant, Φ the potential, and j the index used when summing over all k. The Newton notation for derivatives is used (a dot above a variable indicates the partial derivative with respect to time, while the prime indicates the partial derivative with respect to space), while the divergence reduces to the gradient operator in one dimension (Eq. (1a)). The variables N, c, and $\Phi'$are spatially resolved and thus a function of space, while z, D, and λ are scalars defined by the ion type (and concentrations). The first term on the right-hand side of Eq. (1b) denotes the flux due to diffusion and the second term accounts for migration. Thus, concentration and potential gradient are both driving forces for the ion movement. The mobilities u_k used in the classical Nernst-Planck theory are replaced by the ionic molar conductances, which are connected by $\lambda_k = |z_k| F^2 u_k$. Instead of the Nernst-Planck theory, other models such as the ones mentioned in the introduction can be used to calculate the fluxes. The electroneutrality constraint (Eq. (1c)) is valid for volume elements that have a characteristic size much larger than the Debye length [36] and is evaluated in each volume element of the simulation.

Throughout this work, the combination of Eq. (1a), 1b, and 1c is defined as the system of equation for ion transport models (SoE-ITM). In this SoE-ITM, the Poisson equation can substitute Eq. (1c) to model the electroneutrality of the bulk electrolyte [40–43], which however complicates the solution as elucidated in the '3 Results and Discussion' section. Eq. (1a) and 1b introduce $2k$ equations and $2k$ unknowns (concentrations and fluxes), making the SoE-ITM uniquely determinable if Eq. (1c) is neglected. However, if Eq. (1c) is included in the SoE-ITM, $2k$ unknowns remain while $2k+1$ equations result. This overdetermination is independent of the used flux model. If the potential gradient ϕ' is included as an additional variable, the number of

Table 1
Three examples each for the four different electroneutrality implementations (ENI) denoted here as M1, M2, M3, and M4 found in recent studies with a focus on ion transport in (liquid) electrolytes. M1-M4 are defined in the '2 Methods' section. Only the first author is listed. ENI: Electroneutrality implementation. ITM: Ion transport model. CDD: Concentration dependence of transport parameters. NPt: Nernst-Planck theory. CSt: Concentrated solution theory. SM: Stefan-Maxwell. The asterisk denotes that the codes are available from the authors up on request.

Year	First author	ENI	Electrolyte	ITM	CDD	convection	Code public	Experimental validation
2021	Kim [33]	M1	Multi	diffusion	no	yes	no	no
2017	Rivera [34]	M1	Single	diffusion	no	yes	no	yes
2015	Rivero [35]	M1	Single	diffusion	no	yes	no	yes
2023	Van-Brunt [36]	M2	Multi/ binary	Onsager-SM	no/ yes	no	no*	no
2021	Schammer[27]	M2	Multi	CSt	no	yes	no	yes
2017	Litrico [37]	M2	Multi	NPt	no	yes	no	no
2022	Schalenbach [6,9]	M3	Binary, Multi	NPt	yes	no	yes	yes
2020	Haverkort [38]	M3	Binary	NPt	no	no	no	yes
2013	Akolkar [39]	M3	Binary	CSt	no	no	no	no
2023	León [32]	M4	Multi	NPt	no	yes	no*	yes
2022	Mistry [26]	M4	Binary	CSt	yes	solvent motion	no	no
2021	Colli [10]	M4	Multi	NPt	no	yes	yes	yes

equations and variables both equal $2k+1$.

The calculation of the potential gradient Φ' is often subjected to approximations and misconceptions. In an ideally mixed electrolyte, the potential gradient Φ' is proportional to the local current density (Ohm's law)

$$\Phi' = -\frac{i}{\kappa}, \tag{2}$$

where i denotes the current density, and κ denotes the conductivity. By combining the electroneutrality condition with the Nernst-Planck theory, concentration gradients eventually affect the potential gradient [1]. These extra contributions are commonly denoted as diffusion potentials, which counteract charge separations resulting from different ionic velocities during diffusion. In the current-free case, the diffusion potentials display the differential equivalent to liquid junction potentials which are calculated in the Nernst equation [21,44]. The diffusion potentials as derived for the Nernst-Planck theory (derivation in the Supporting Information) add to Ohm's contributions of the potential gradient [1] from Eq. (2):

$$\Phi' = -\frac{i}{\kappa} - \frac{F}{\kappa}\sum_j D_j z_j c'_j \tag{3}$$

Therefore, while using the Nernst-Planck theory, Eq. (1c) can be substituted with Eq. (3), leading to

$$c_k{}' = -N'_k \qquad \forall k \tag{4a}$$

$$N_k = -D_k c'_k - \frac{z_k \lambda_k}{|z_k| F} c_k \Phi' \quad \forall k \tag{4b}$$

$$\Phi' = -\frac{i}{\kappa} - \frac{F}{\kappa}\sum_j D_j z_j c'_j. \tag{4c}$$

The SoE-ITM of Eq. 4 automatically satisfies the electroneutrality constraint.

2.2. Electroneutrality implementations

For the comparison of the four different implementation methods M1 to M4, an ion transport model is evaluated, which is implemented in Python (see Supporting Information). The model procedure is depicted in Fig. 1. The model is calculated in just one direction (in the following referred to as 'one-dimensional'). The four implementation methods for the electroneutrality constraint (ENC) compared within this study are summarized and compared in Table 2.

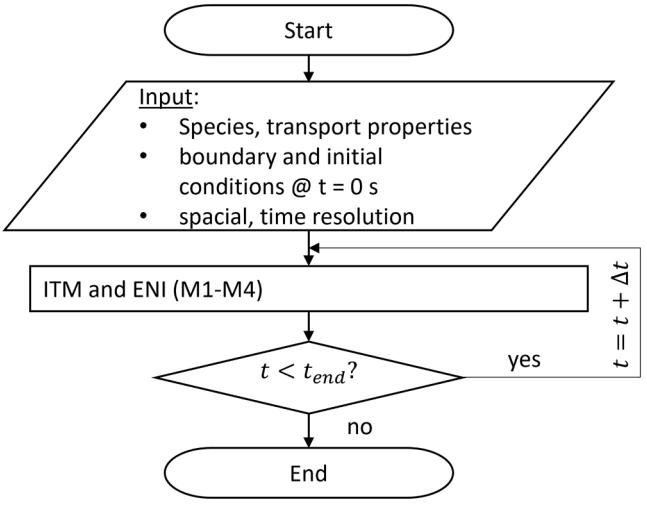

Fig. 1. General simulation framework for the comparison of methods to enforce electroneutrality in ion transport models. ITM: ion transport model. ENI: Electroneutrality implementation.

Fig. 2 shows a simplified schematic of the methods M1 to M4 (top to bottom) for the case of a diffusing binary electrolyte. The concentration on the left-hand side is higher than on the right-hand side. The black arrows indicate the fluxes of the ions as described in Step 2 in Table 2. The red arrows symbolize how the electroneutrality is enforced (Step 3). In the following, the used models M1 to M4 are discussed in detail.

Method M1: ENC neglected – The ion transport is calculated with Eq. (1a) and Eq. (1b) individually without considering the ENC. Hence, diffusion potentials and any interactions between the ions are neglected. This approach is used for instance in references [33–35]. For k fluxes, k equations are solved (Eq. (1b)) that determine the k concentrations using Eq. (1a). So, in total $2k$ equations determine $2k$ unknowns.

Method M2: ENC solved explicitly – The transport of all ions except ion type m is calculated individually using the flux equations like in method M1. Instead of calculating the distribution of the ion type m based on a flux by the Nernst-Planck model, it is calculated to fulfil electroneutrality (Eq. (1c)):

$$c_m = -\frac{1}{z_m}\sum_{j,j\neq m} z_j c_j \,. \tag{5}$$

Hence, the transport properties of ion type m are neglected and this type of ion just serves as a filler to counteract the electroneutrality gaps left by the movement of the other ions. To calculate the ion transport of the other ions, Eq. (1a) and Eq. (1b) (for all k but not for m) are solved resulting in total $2(k-1)$ equations for the fluxes and ion concentrations $c_{k\neq m}$. Together with Eq. 5, in total $2k-1$ equations and $2k-1$ variables exist since the flux for m is not determined. This method has been used by references [37,45] and is typical for concentrated solution theories [1,36]. Volgin et al. [46] discussed that towards larger numbers of ion species this approach shows an increasing error of the modelled ion transport.

Method M3: Secondary fluxes – The ion transport is calculated using the flux equations, which may result in local charge accumulations (like M1). These local charge accumulations are balanced in a second, subsequent step by so called secondary fluxes N_k^{**} for every ion species. Method M2 is a special case of M3, where all except one secondary fluxes equal zero. In the following, the definition of N_k^{**} used in this work will be elucidated. Based on Faraday's law, the current density i^* due to primary ion transport N_k^* is defined by [1]:

$$i^* = F\sum_j z_j N_j^* \,. \tag{6}$$

The asterisk denotes the hypothetical currents and fluxes after the primary calculated ion transport by Eq. (1a) and Eq. (1b). The one-dimensional continuity equation for electrical charges is

Table 2
Short description and calculation steps of methods M1-M4 being assessed in this study. Methods M1-M4 describe different approaches to incorporate the electroneutrality constraint (ENC) in ion transport models.

	description	Step 1: Φ'	Step 2: fluxes	Step 3: electroneutrality
M1	ENC neglected	Eq. (2)	Eq. (1b) $\forall k$	(none)
M2	ENC solved explicitly	Eq. (2)	Eq. (1b) $\forall k$, $k \neq m$	Eq. (5) for m
M3a	secondary fluxes	Eq. (2)	Eq. (1b) (diffusion) $\forall k$	Eq. (11) $\forall k$, Eq. (2) (migration) $\forall k$
M3b	secondary fluxes	Eq. (2)	Eq. (1b) $\forall k$	Eq. (11) $\forall k$
M4	potential dependent calculation	Eq. (3)/4c	Eq. (1b)/4b $\forall k$	(implicit by Eq. (3)/4c)

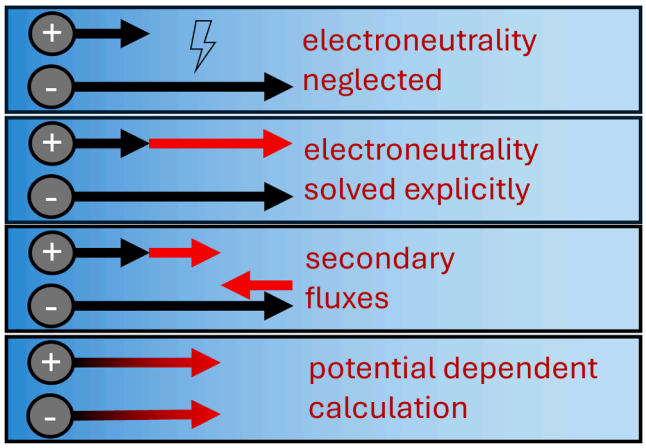

Fig. 2. Abstraction of methods M1 to M4 for the case of pure diffusion. The black arrows indicate the individual flux of the ion types, while the red arrows show the effect of the ENI on the calculated flux.

$$\frac{\partial q}{\partial t} + i^{*'} = 0, \tag{7}$$

where q defines the charge density. If the divergence of i^* differs from zero, charge accumulates leading to electric fields (Poisson's equation). To equalize these electric fields, a secondary transport of ions is introduced with a current density i^{**}. The divergence of the sum of the primary and secondary current densities must equal zero so that local charges do not accumulate (Eq. (7), $\partial q/\partial t = 0$). This condition ensures that the ENC remains fulfilled ($q = 0$). For the case of the one-dimensional model, this condition simply implicates that the current densities in all cells equal the applied total current density i_{total}:

$$(i^* + i^{**}) = i_{\text{total}}. \tag{8}$$

Based on Faraday's law, the secondary current densities are proportional to the fluxes, so that normalizing the secondary current densities yields:

$$\frac{i_k^{**}}{i^{**}} = \frac{z_k N_k^{**}}{\sum_j z_j N_j^{**}}. \tag{9}$$

Based on the Nernst-Planck theory, the flux N_k^{**} of each ion driven by the electrical field is proportional to its ionic molar conductivity. By inserting this relation into Eq. (9), the partial current densities become a function of the conductivities:

$$\left|\frac{i_k^{**}}{i^{**}}\right| = \frac{c_k \lambda_k}{\sum_j c_j \lambda_j}. \tag{10}$$

By combining Eq. (9) and Eq. (10), the secondary flux of species k can be calculated by

$$N_k^{**} = -i^{**} \frac{\lambda_k c_k}{F z_k \sum_j c_j \lambda_j}. \tag{11}$$

The total flux after applying the secondary fluxes is:

$$N_k = N_k^* + N_k^{**}. \tag{12}$$

The secondary fluxes as defined in Eq. (11) mimic the ion transport due to diffusion potentials, as discussed in the Supporting Information in detail.

M3 can be distinguished into two subcategories: (i) In **M3a**, the diffusion is calculated, and the secondary fluxes are subsequently included. In a third step, the potential gradient driven migration (Eq. (2)) is calculated, as pure migration does not introduce deviations from electroneutrality. In a binary case, the effective diffusion of both ions after the correction using secondary fluxes coincides with mutual diffusion [47]. The fractional step algorithm by Kwok et al. [48] can be categorized as M3a. (ii) In **M3b**, the diffusion and migration are calculated, followed by including the secondary fluxes. M3b is discussed and used by Volgin et al. [49], and Schalenbach et al. [9,50], respectively. The outcomes of M3a and M3b are similar (except numerical errors) and are therefore not distinguished in the results section.

Method M4: Potential dependent calculation – In this method, the potential gradient is calculated as a dependent variable. Instead of SoE-ITM of Eq.1, SoE-ITM of Eq. 4 is used which is equivalent but includes the potentials explicitly. Hence, in the SoE-ITM the number of both, variables and equations equal $2k + 1$, providing a uniquely determinable solution of the potential gradient, k fluxes and k ion concentrations. Two approaches can be distinguished within this method: (i) using the ENC to calculate the potential gradient, used for example by Bauer et al. [8,12,51], and Colli et al. [10]; (ii) using the Poisson equation to calculate the potential gradient, often referred to as Poisson-Nernst-Planck, or Nernst-Planck-Poisson equations. This approach and is used and studied intensely in the literature [52,53]. In this study, M4 is implemented with the first approach, as the second is mathematically more complex. Similarities and differences of both approaches are briefly discussed in the '3 Results and Discussion' section.

2.3. Electrochemical setups and parameterization

In this study, the ion transport is modelled for the five different electrochemical setups (S1 to S5) shown in Table 3, aiming to demonstrate and analyse the effect of each electroneutrality implementation method in detail. The phenomenological complexity in the setups increases, aiming a separate examination of different contributions to the ion transport. The computational domain is a one-dimensional array of 50 equisized cells. The time increment is $\Delta t = 0.1$ s and a forward Euler scheme is used. The simulation results are shown for a simulation time of 1800 s except for the ternary system (1300 s) due to the lower limiting current, and earlier educt starvation at the cathode [9].

For the setups S1 to S4, a concentration-independent parameterization of diffusivity, and molar conductivity is used. The diffusion coefficients for H^+, Cl^-, Cu^{2+}, SO_4^{2-}, and Na^+at infinite dilution are used with values of 9.312, 2.032, 0.72, 1.065, and 1.334 (10^{-5} cm^2/s) at 25 °C, respectively [1]. The conductivities and diffusion coefficients are related by $RT\lambda_k = D_k|z_k|F^2$ using the Nernst-Einstein equation ($D_k = RTu_k$). In case of setup S5, a concentration-dependent parameterization for $CuSO_4$ is implemented using experimental data from references [54–58]. The temperature dependence of the diffusion coefficient presented by Moats et al. [59] is adapted to adjust the temperature of the parameterization (at 25 °C) to the data used for the evaluation of the transport model in reference [6] at a temperature of 20 °C.

3. Results and discussion

3.1. Thought experiments with simplistic parameterizations

In the subsequent analysis, the influences of the four different electroneutrality implementations (ENIs) M1 to M4 (introduced in the methods section) on ion transport modelling are discussed using simplistic parameterizations. These parameterizations represent

Table 3
Characteristics of simulated setups considered within this work. All electrolytes are aqueous. d: distance between electrodes. CDD: concentration dependence.

Setup	Electrolyte	d (mm)	i (mA/cm^2)	CDD
S1	0.1 M HCl / 0.1 M $CuSO_4$	7.1	0	No
S2 (Hittorf)	0.1 M HCl	>100	0.75	No
S3a	0.1 M HCl	7.1	0.75	No
S3b	0.1 M $CuSO_4$	7.1	1.50	No
S4	0.1 M $CuSO_4$ + 0.1 M Na_2SO_4	7.1	1.50	No
S5	0.1 M $CuSO_4$	7.1	1.50	Yes

hypothetical experiments within one-dimensional simulations of a static electrolyte (no convection) and concentration independent diffusion coefficients, mobilities, and conductivities. The results of calculations using the different methods is colour coded: method M1 is depicted in blue, M2 in red, M3 in green, and M4 in orange. The meaning of the line styles is not general but varies for better distinguishability and is explained in every plot, respectively.

Diffusion at a concentration step – Fig. 3A shows the initial concentration profile of a step function, with 0.2 M HCl on the left side and 0.2 mM on the right side, resembling the electrochemical setup S1 described in Table 3. The equilibrations of the concentration profiles are calculated with the ion transport model for the four different ENIs and plotted for a simulation time of $t = 1800$ s. Calculating H^+ using M1 (the considered species are evaluated individually using their respective flux equations) results in an almost equilibrated concentration profile. For Cl^-, the 4.6-times lower diffusion coefficient than that of H^+ leads to a concentration profile with larger differences. For M2 (solving the electroneutrality constraint explicitly), the resulting concentration profiles of both ions overlap with either the cation using M1 (shown in the figure), or the anion using M1, depending on the choice which ion is calculated *via* Eq. (3). M3, and M4 show overlapping concentration profiles that deviate from the profiles using M1 or M2.

In Fig. 3B, the absolute value of the normalized charge density $|Q/Q_{+,0}|$ from the simulations in Fig. 3A is graphed at a simulation time of $t = 1800$ s, with the charge density Q and the averaged initial charge density of the cations $Q_{+,0}$. The different mobilities of $H^+$and Cl^- lead to a large charge separation along the setup for M1. For M2 the charge densities are exactly zero. For M3 the charge density is non-zero only in the last cell due to the secondary fluxes. M4 shows normalized charge densities lower than about 10^{-15}, which correlates to the expectable numerical error.

Fig. 3C represents the same thought experiment but with $CuSO_4$ instead of HCl. The cations and anions separate using M1, like the data shown in Fig. 3A. However, with $CuSO_4$, the diffusion coefficients of the anion and cation are only slightly different (cation 32 % slower that anion), for which the differences of the calculated concentrations with the different ENIs are less pronounced. Using M2 to calculate the sulphate ion concentration results in a slower transport than predicted by its flux equation (M1). M3 and M4 are overlapping in between both concentration profiles using M1 (blue).

Fig. 3D shows $|Q/Q_{+,0}|$ for the simulated profiles of Cu^{2+} and SO_4^{2-} shown in Fig. 3C. As for HCl, the different mobilities of the anions and cations results in charge separation using M1. For the other methods, $|Q/Q_{+,0}|$is below 10^{-14}. For $CuSO_4$ the general trends are like HCl, but the normalized charge densities are smaller due to the smaller difference of the mobilities (and smaller total mobilities). Overall, except M1 all methods enforce electroneutrality reasonably.

Hittorf model – Setup S2 resembles a computational portray of the Hittorf apparatus [60] that is typically used to experimentally determine transference numbers (the fractions of current carried by each ion). Ideally, the concentration inside the reactor is constant except directly at the electrode. The results of simulations of setup S2 are shown in Table 4 considering HCl. If H^+ is calculated *via* Eq. (1b) (Nernst-Planck) enforcing the current, the transference number of H^+ is 22 % too high. Doing the same for Cl^-, the transference number is >5-fold the real data.

Electrochemistry ***of a binary electrolyte*** - Fig. 4A shows the concentration profiles for S3a, a simulation in which a constant current is applied to an initially equilibrated solution of HCl. H^+ and Cl^- are consumed at the electrodes (H_2 and Cl_2 evolution reactions). As both $H^+$and Cl^- are consumed at the electrodes, their concentration decreases at the electrochemical interfaces which impact the entire concentration in the solution over time. Due to the lower mobility of Cl^-, the concentration decreases faster at the anode than H^+ at the cathode. Like in the case of pure diffusion, the difference between the ion mobilities leads to deviations between the simulated concentration profiles when a

Table 4
Expectable deviations of transference number (Hittorf) for HCl from theoretical values when the transference number are calculated from the results of transport simulations with the respective methods. H^+/Cl^-.

Property (experiment)	$t_{simulation}$ / t_{input}
M1	0
M2	1.22 (H^+); 5.58 (Cl^-)
M3	0
M4	0
M5	0

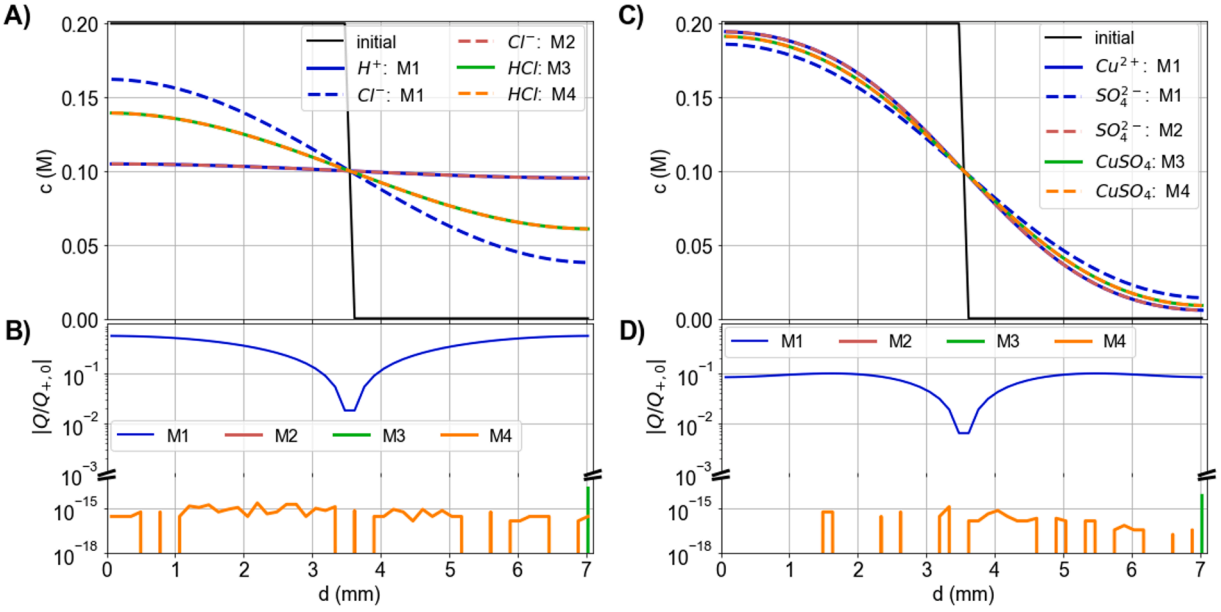

Fig. 3. Simulated concentration profiles (A, C) and normalized absolute charge density (B, D) after an initial concentration step and equilibration by diffusion, resembling setup S1. Concentration profiles of M1 and M2 deviate from M3 and M4. The expectable numerical error for the normalized absolute charge density is about 10^{-15}. All methods except M1 enforce reasonable electroneutrality.

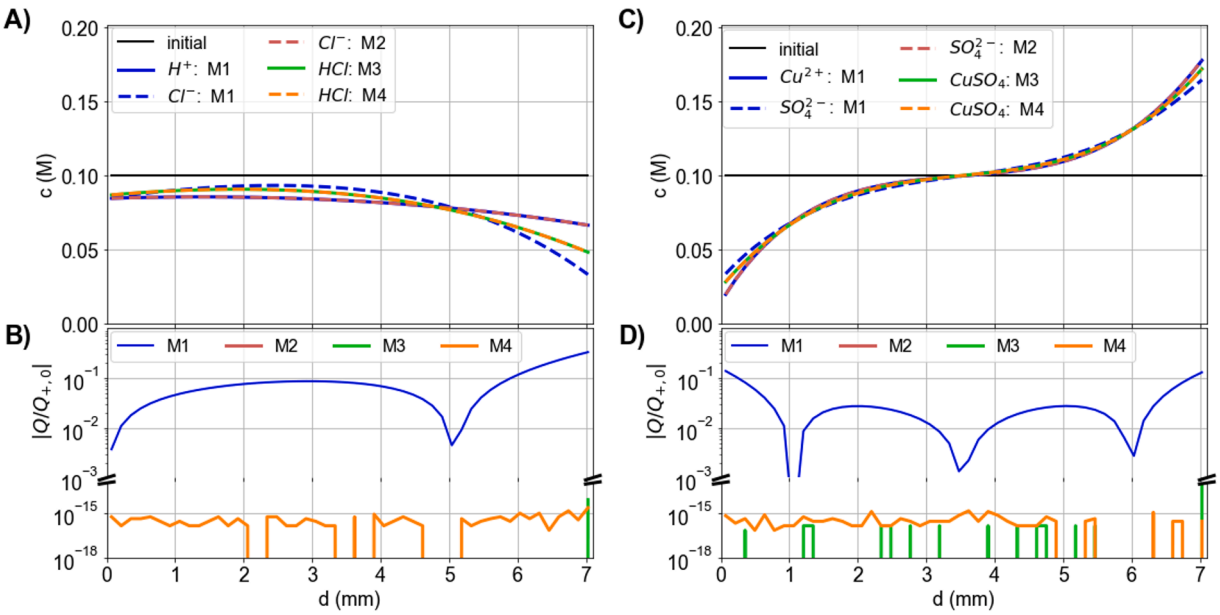

Fig. 4. Concentration profiles (A, C) and normalized absolute charge density (B, D) for setup S3a (HCl) and S3b ($CuSO_4$), respectively. Concentration profiles of M1 and M2 deviate from M3 and M4 (as in S1). The expectable numerical error for the normalized absolute charge density is about 10^{-15}. All methods except M1 enforce reasonable electroneutrality.

current is applied to a system and the electroneutrality is neglected (M1, blue). The concentration profiles simulated with M3 and M4 show values between those of the anions and cations of M1.

Fig. 4B shows the ratio $|Q/Q_{+,0}|$ related to the simulated concentration profiles in Fig. 4A. Like the case of the diffusion in Fig. 3B, M1 shows a significant deviation from electroneutrality, M2 is perfectly electroneutral, while for M3 and M4 the magnitude of the charge differences is within the range of the expectable numerical error. Fig. 4C and 4D show the simulated concentration profiles and the normalized absolute charge density for S3b, a simulation in which a constant current is applied to an initially equilibrated solution of $CuSO_4$ (copper deposition and dissolution), respectively. The current is twice as high as in S3a so that the number of cations reacting is similar. In contrast to S3a, the concentration in S3b stays constant during the process, as the number of cations consumed at the cathode is equal to that introduced into the electrolyte at the anode. Although the concentration profiles are rather close together for all methods (Fig. 4C), the respective deviation from electroneutrality shown in Fig. 4D is significant for M1. M2 to M4 implement electroneutrality reasonably.

Electrochemistry of multi-ion electrolytes - Method M1 and M2 were found to be barely used for binary electrolytes in the literature [33], while they display often employed ENIs for multi-ion electrolytes and are suggested for multi-ion simulations in textbooks [1]. Fig. 5 shows the simulated concentration profiles of Na^+, Cu^{2+} and SO_4^{2-} in S4 using M1, M2 and M3 for a multi-ion electrolyte (the profiles using M4 overlap with M3). Like discussed in the '2 Methods' section, the outcome of M2 depends on the choice of the ion type that balances the charge *via* Eq. (5). In Fig. 5, the result for the concentration profile of Na^+ using M2 are M2 the same as those using M1 if Cu^{2+} or SO_4^{2-} are chosen as the ion type for the charge balance (Eq. (5)). However, when choosing Na^+ itself, its concentration profile differs from that of method M1. These findings for M2 are directly applicable to $Cu^{2+}$and SO_4^{2-}, respectively. Similar insights have been also discussed by Volgin et al. [49], who also discussed that the results of the concentration profiles depend on the choice of the ion type that is used for the charge balance in M2. The resulting three concentration profiles of each species deviate for each method, respectively.

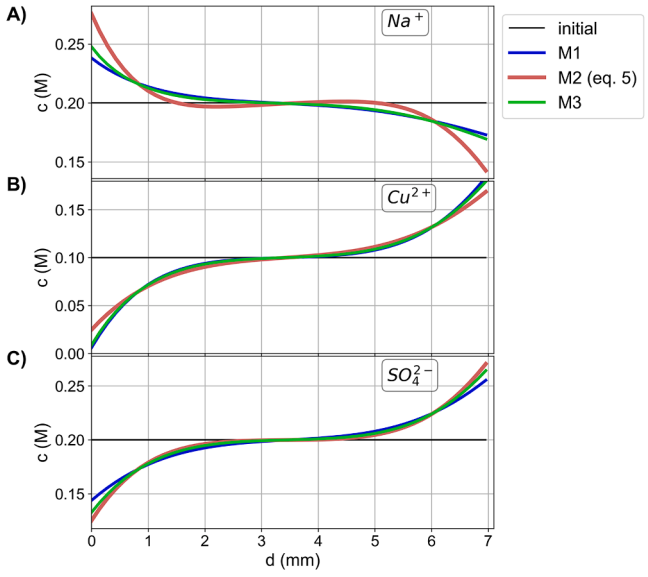

Fig. 5. Simulated concentration profiles in the multi-ion setup S4. A) Sodium ions. B) Copper ions. C) Sulphate ions. In M2, the profiles of the ion types that are not calculated via Eq. (5) correspond to M1. Therefore, each brown concentration profile (M2) of one ion type corresponds to the blue lines for the other ion types. With method M2, the choice of the ion solved via the electroneutrality constraint significantly affects the results.

3.2. *Experimental validation*

Unlike the thought experiments above, concentration-dependent parameterizations must be used to portray real electrolytes and to make a meaningful evaluation of the simulations with experiments. Method M1, as shown above, violates electroneutrality, making it unsuitable for describing any experimental data. In the case of M2, different results were obtained depending on the choice of ion, indicating that this method cannot reliably describe any experimental data. Hence, these approaches are not considered in the following

experimental evaluation of the influence of the electroneutrality constraint. For ternary electrolytes concentration-dependent parametrizations based on experimental data are rarely available. Therefore, the ENIs of method M3 and M4 will be considered for the binary $CuSO_4$ solution and compared to experimental data from the literature [6].

Fig. 6A shows the simulated concentration profiles for setup S5 with respect to a simulation time of 1800 s using concentration-dependent (cyan line) and concentration-independent (purple line) parameterizations. The concentration profiles are independent of the used electroneutrality methods (M3/M4), and the concentration profiles show a rather small difference regarding the concentration dependence. Here, the area resistance is used a sensitive metric to compare measured and simulated data in Fig. 6B. From the experimental side, the area resistance comes with the advantage of high measurement precision, while physicochemical-wise the depletion of ions near the cathode (Fig. 6A) leads to a large impact on this metric. The concentration-independent parameterization deviates significantly from measurement data after about 1000 s, as it does not portray the physicochemical properties of the electrolyte. In contrast, with the concentration-dependent parameterization, an exact match to the experimental data is achieved.

3.3. Assessment

Except method M1, all methods ensure electroneutrality within the computational domain. However, for method M2, the simulated concentration profiles are subjected to an arbitrary choice of the ion species. Methods M3 and M4 led to similar results. In the following assessment, the differences of methods M1 to M4 to calculate the electroneutrality constraint in transport modelling are discussed regarding their mathematical background and physicochemical implications. Table 5 summarizes important characteristics of the discussed methods.

Mathematical comparison - Here, the one-dimensional case was considered as a simple model system to focus on common methods to introduce the electroneutrality implementations for the ion transport,

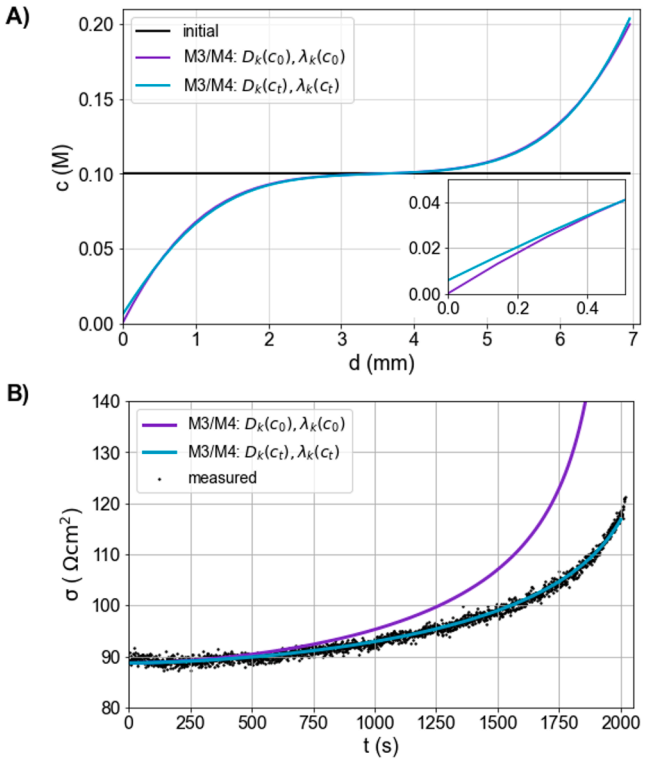

Fig. 6. Simulation and measurement data of S5. A: concentration profiles after t = 1800 s; B: area resistance over time. Measurement data from Schalenbach et al. [6].

avoiding the complexity issues arising with the multi-dimensional cases [12]. In the cases of M1 and M3, the electroneutrality constraint (Eq. (1c)) was not involved in the initial application of the ion transport calculation. For M3, Eq. (1c) is considered in a separated simulation step. For the case of method M2, one transport equation is neglected and substituted with Eq. (1c). Hence, methods M1, M2, M3 display workarounds to match the number of concentrations to the number of equations, avoiding the overdetermination of SoE-ITM Eq. 1 that arises due to the fixed potential gradient based on Ohm's law. If the potential gradient is assumed as a dependent variable, the contributions of the diffusion potentials are included (Eq. (3)). Hence, the SoE-ITM of Eq. 4 for method M4 was derived, in which the total $2k+1$ variables meet $2k+1$ equations. As a benefit, the electroneutrality implementation is included into the direct solution of the SoE-ITM of Eq. 4 by the diffusion potentials. In the one-dimensional case discussed thus far each volume element of the used discretization comes with two faces. Consequently, all computational cells are in serial and the current is constant throughout the computational domain, making the computation of the potential gradient (Eq. (2), or Eq. (3)) straight-forward.

In the multi-dimensional case (SoE-ITM provided in the Supporting Information), the current is in general unknown because the current runs in serial and parallel through the electrolyte. To obtain the potential gradients and the current densities for methods M1, M2, and M3 with Eq. (2), a current network must be solved in which the resistances are determined by the concentrations (that determine the conductivities). Then, the ion fluxes are determined based on the concentrations of the previous time iteration step and potential gradients. For the three-dimensional case, the number of faces n_f for each volume element increases depending on the discretization. For instance, in the case of cubic discretization, each volume element shows $n_f = 6$ faces. The fluxes and potential gradients of one face serve for two volume elements, so that $n_f/2$ fluxes must be determined for every cubic volume element. In case of M1, M3, and M4, a total number of k times $n_f/2$ fluxes and k concentrations must be determined for each volume element, resulting in a total amount of $k(n_f/2+1)$ variables. With reference to the SoE-ITM of Eq. 1 (without the electroneutrality condition), the number of equations is also $k(n_f/2+1)$. Analogously, in the case of M2 the number of fluxes reduces to $k-1$ per face, but Eq. (1c) needs to be solved, leading to $(k-1)(n_f+1)+1$ variables and equations.

For M4, the potential gradients at the volume element faces are influenced by both the current and the concentration gradients (see Eq. (3)), requiring dependent computations. This dependency requires $n_f/2$ equations of type Eq. (3) in addition to that of M1 and M3. Therefore, the total number of unknowns and equations is $k(n_f+1)$. Solving the arising system of equation is challenging due to the impact of concentration gradient and current on the potential gradient (see Eq. (3)), which results in interdependent fluxes, current densities and potential gradients. In other words, the resistor network used in methods M1 and M3 to calculate potential gradients and currents now also depends on the fluxes to be solved. Consequently, a general analytical solution for M4 does not exist, and numerical approaches to solve the system of equations require an iterative solver, which is computationally expensive. Various researchers tried to overcome the difficulties of multi-dimensional systems using different approaches, simplifications, and analogies. Pillay et al. [61] defined a quasi-potential approach for steady-state calculations which may be categorized as M4. Sarkar et al. [62] resolved the electroneutrality constraint by introducing a Lagrange multiplier that accounts for the ion-ion interactions during ion transport. Katagiri [63] uses an analogy to steady-state heat-transfer equations to resolve the potential.

To summarize, for the one-dimensional case method M4 is considered by the authors as the most elegant mathematical solution for the ion transport. However, in the multi-dimensional case, conducting M4 is limited by the computational efforts that arise from the variable interactions. Hence, M3 seems a reasonable alternative to ease the

Table 5
Assessment by comparison of the capability and accuracy of simulation features using the different ENIs. *Regarding the transport. ** Up to defined error tolerance. ***may increase computational effort.

Method	Multi-ion capability	EN fulfilled	Diffusion potentials	Hittorf/ Diffusion validation	c-dependence meaningfully integrable	Possible transport accuracy	Computational effort
M1	Yes	No	No	Yes/No	Barely	Low	Low
M2	Yes	Yes	No	No/No	No	Low	Low
M3	Yes	Yes	(Yes*)	Yes/Yes	Yes	High	Low
M4	Yes	Yes**	Yes	Yes/Yes	Yes***	High	High

modelling of ion transport. In the literature [40–43], the algebraic electroneutrality constraint of Eq. (1c) is often replaced with the Poisson equation (an elliptic partial differential equation). The solution of the so called Poisson-Nernst-Planck or Nernst-Planck-Poisson equations is challenging and requires special numerical solvers due to the arising stiff system of equations [41,42].

Physicochemical differences **-** Methods M1 and M2 do not display the physics of ion transport properly as shown in Fig. 3-5 and Table 4. M1 does not enforce electroneutrality while the calculated transport using M2 depends on an arbitrary choice. Hence, they will not be discussed in more detail.

The concentration profiles using methods M3 and M4 are similar. Therefore, M3 and M4 predict the same ion transport. In the Supporting Information, it is shown that methods M3 (using Eq. (11)) and M4 coincide exactly for the case of pure diffusion. However, diffusion potentials are neglected using M3, while the transport due to the unknown diffusion potentials is calculated *via* Ohm's and Faraday's laws (Eq. 11). Fig. 7 shows the simulated cell-voltage over time for M3 and M4 with setup S5. The simulated cell voltage with method M4 shows higher values than that with M3. The difference between the two voltages of up to 25 mV are due to the diffusion potentials. For applications involving high concentration gradients, method M4 is necessary to accurately predict the potentials. To minimize the influence of diffusion potentials, the conductivity of the solution can be increased by adding supporting electrolytes, and concentration gradients can be reduced through natural or forced convection. Therefore, in multi-component processes that involve convection, such as electrowinning, the effect of diffusion potentials can often be neglected, allowing the use of M3 instead of M4 with minimal impact on the calculated voltage.

Using M4, the electroneutrality constraint governs and alters the electrical field [48], although it is a mathematical confinement and not a physical law. Sarkar et al. [62] argues that the combination of Nernst-Planck equations and electroneutrality constraint is physically incompatible as the former assumes no interactions between the ions (similar to an ideal gas) but the latter enforces interactions. Sarkar et al. also criticize that the results do not necessarily satisfy Gauss' law ($\nabla^2\Phi = 0$). However, this fact is due to the considered concentration gradients and the respective diffusion potentials [64]. Assuming that a superposition of the field due to diffusion potentials and the field due to external excitation is accurate implicates a physically meaningful solution. Although it should be noted that an intrinsic contradiction occurs: Differentiating Eq. (3) (under neglection of i) gives a non-zero term on the right-hand side that corresponds to a charge density considering the Poisson equation. Detailed discussions on that topic are given by Mafé et al. [64–66]. Briefly, if the concentration gradient is not extremely high and the thickness of the diffusion junction is significantly bigger than the Debye length, then the arising charge density is negligible. This is usually the case for the discretization of a macroscopic reactor using finite volumes but excludes the double layer.

With the Poisson equation the physical representation of the electroneutrality condition can be implemented in the Nernst-Planck model instead of using the electroneutrality constraint (Eq. (1c)) that is indirectly justified with the Poisson equation. However, the charge density that is expected in real systems is vanishingly small (although leading to diffusion potentials) due to the strong electric forces. Therefore, a benefit for calculations of liquid electrolytes is not to be expected using the Poisson equation. For liquid electrolytes, the significance of the Poisson equation is restricted to very small length scales such as the double layer [18]. The effect of coulombic interactions is ultimately covered within diffusion potentials on a length scale typical for macroscopic models of electrochemical reactors. Therefore, the electroneutrality constraint is a good macroscopic approximation of the microscopic n-body problem.

To conclude, from a physicochemical perspective, method M4 is considered the best among the four discussed methods to implement the electroneutrality constraint, as it ensures accurate ion transport predictions, maintains charge balance, and provides a realistic potential gradient. Alternatively, on the cost of non-correctly modelled potential distribution due to neglecting diffusion potentials, method M3 can be used to accurately model the concentration gradients and ion fluxes.

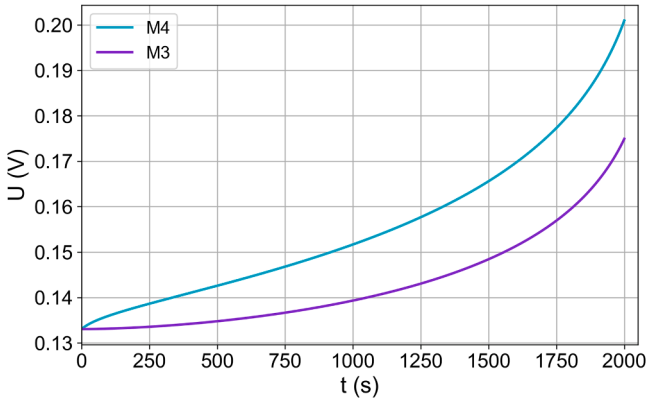

Fig. 7. Calculated voltage as the driving force for the ion transport in S5. The potential gradient of M3 is based on Ohm's law while M4 includes diffusion potentials.

4. Conclusion

In this study, four different methods from the literature to implement the electroneutrality constraint in ion transport models are compared. For this purpose, a simple one-dimensional framework is used to evaluate the physical properties such as the effective transport (by means of concentration profiles), charge accumulations, the area resistance, and the calculated potential field. The method to enforce electroneutrality in electrochemical transport models is shown to have significant influence on the simulation outcome, including computational effort and predicted transport. Some methods to implement electroneutrality lead to unphysical charge accumulations or imprecise ion transport. With proper implementation of the electroneutrality condition, ion transport models are highlighted to accurately represent experimental data.

List of symbols

c	concentration
d	distance
D	diffusion coefficient

(*continued on next page*)

(*continued*)

F	Faraday constant
i	current density
j, k	indices for species
L	proportionality constant
N	flux
Q	charge density
R	gas constant
t	time
t_j	transference number
T	temperature
u	mobility
z	valence
Φ	(electrostatic) potential
μ	electrochemical potential
μ^*	chemical potential
λ^0	Ionic equivalent conductivity
λ	Ionic molar conductivity
κ	conductivity
CSt	Concentrated solution theory
CDD	concentration dependent
ENC	electroneutrality constraint
NPt	Nernst-Planck theory
SoE	System of equations
SoE-ITM	System of equations for ion transport models

CRediT authorship contribution statement

Benjamin Janotta: Writing – original draft, Visualization, Software, Methodology, Conceptualization. **Maximilian Schalenbach:** Writing – original draft, Visualization, Supervision, Methodology, Funding acquisition, Conceptualization. **Hermann Tempel:** Writing – review & editing, Project administration, Funding acquisition. **Rüdiger-A. Eichel:** Project administration, Funding acquisition.

Declaration of competing interest

The authors declare that they have no known competing financial interests or personal relationships that could have appeared to influence the work reported in this paper.

Acknowledgement

This work was supported by the German Federal Ministry of Education and Research (BMBF) within the Project PRELUDE (03SF0650A).

Supplementary materials

Supplementary material associated with this article can be found, in the online version, at doi:10.1016/j.electacta.2024.145280.

Data availability

The data will be available online on gitlab.

References

[1] J.S. Newman, N.P. Balsara, Electrochemical Systems, John Wiley & Sons, Inc, Hoboken, 2021.
[2] A.J. Bard, L.R. Faulkner, Electrochemical methods: Fundamentals and Applications, 9th ed., Wiley, New York, 1980 [u.a.].
[3] M. Schalenbach, Y.E. Durmus, H. Tempel, H. Kungl, R.A. Eichel, A Dynamic Transmission Line Model to Describe the Potential Dependence of Double-Layer Capacitances in Cyclic Voltammetry, J. Phys. Chem. C 125 (2021) 27465–27471, https://doi.org/10.1021/acs.jpcc.1c08595.
[4] P.S. Crozier, R.L. Rowley, D. Henderson, Molecular dynamics calculations of the electrochemical properties of electrolyte systems between charged electrodes, J. Chem. Phys. 113 (2000) 9202–9207, https://doi.org/10.1063/1.1320825.
[5] S. Feldberg, On the dilemma of the use of the electroneutrality constraint in electrochemical calculations, Electrochem. commun. 2 (2000) 453–456, https://doi.org/10.1016/S1388-2481(00)00055-2.
[6] M. Schalenbach, B. Hecker, B. Schmid, Y.E. Durmus, H. Tempel, H. Kungl, R.A. Eichel, Ionic transport modeling for liquid electrolytes - Experimental evaluation by concentration gradients and limited currents, Electrochem. Sci. Adv.. https://doi.org/10.1002/elsa.202100189.
[7] A. Mistry, V. Srinivasan, Do we need an accurate understanding of transport in electrolytes? Joule 5 (2021) 2773–2776, https://doi.org/10.1016/j.joule.2021.10.007.
[8] G. Bauer, V. Gravemeier, W.A. Wall, A stabilized finite element method for the numerical simulation of multi-ion transport in electrochemical systems, Comput. Methods Appl. Mech. Eng. 223-224 (2012) 199–210, https://doi.org/10.1016/j.cma.2012.02.003.
[9] M. Schalenbach, Y.E. Durmus, H. Tempel, H. Kungl, R.A. Eichel, Ion transport and limited currents in supporting electrolytes and ionic liquids, Sci. Rep. 12 (2022) 6215, https://doi.org/10.1038/s41598-022-10183-2.
[10] A.N. Colli, J.M. Bisang, Tertiary Current and Potential Distribution Including Laminar/Turbulent Convection, Diffusion, and Migration by the Finite Volume Method Using OpenFOAM, Ind. Eng. Chem. Res. 60 (2021) 11927–11941, https://doi.org/10.1021/acs.iecr.1c01884.
[11] A.N. Colli, J.M. Bisang, Combination of Cumulative and Convergent Flows as a Means to Improve the Uniformity of Tertiary Current Distribution in Parallel-Plate Electrochemical Reactors, J. Electrochem. Soc. 164 (2017) E42–E47, https://doi.org/10.1149/2.0521704jes.
[12] G. Bauer, A Coupled Finite Element Approach For Electrochemical Systems. München, Technische Universität München, München, 2012. Diss2012.
[13] R.E. Palma-Goyes, F.F. Rivera, J. Vazquez-Arenas, Heterogeneous Model To Distinguish the Activity of Electrogenerated Chlorine Species from Soluble Chlorine in an Electrochemical Reactor, Ind. Eng. Chem. Res. 58 (2019) 22399–22407, https://doi.org/10.1021/acs.iecr.9b05185.
[14] M. Spasojević, N. Krstajić, P. Spasojević, L. Ribić-Zelenović, Modelling current efficiency in an electrochemical hypochlorite reactor, Chemical Engineering Research and Design 93 (2015) 591–601, https://doi.org/10.1016/j.cherd.2014.07.025.
[15] A.N. Colli, J.M. Bisang, Current and Potential Distribution in Two-Phase (Gas Evolving) Electrochemical Reactors by the Finite Volume Method, J. Electrochem. Soc. 169 (2022) 34524, https://doi.org/10.1149/1945-7111/ac5d90.
[16] F.F. Rivera, T. Pérez, L.F. Castañeda, J.L. Nava, Mathematical modeling and simulation of electrochemical reactors: A critical review, Chem. Eng. Sci. 239 (2021) 116622, https://doi.org/10.1016/j.ces.2021.116622.
[17] R.C. ALKIRE, SPECIAL REVIEW TRANSPORT PROCESSES IN ELECTROCHEMICAL SYSTEMS, Chem. Eng. Commun. 38 (1985) 401–413, https://doi.org/10.1080/00986448508911318.
[18] J. Newman, Fundamental mathematical principles for electrochemical engineering, 1983.
[19] W. Nernst, Zur Kinetik der in Lösung befindlichen Körper, Zeitschrift für Physikalische Chemie 2U (1888) 613–637. https://doi.org/10.1515/zpch-1888-0274.
[20] M. Planck, Ueber die Erregung von Electricität und Wärme in Electrolyten, Ann. Phys. 275 (1890) 161–186, https://doi.org/10.1002/andp.18902750202.
[21] M. Planck, Ueber die Potentialdifferenz zwischen zwei verdünnten Lösungen binärer Electrolyte, Ann. Phys. 276 (1890) 561–576, https://doi.org/10.1002/andp.18902760802.
[22] L. Onsager, Reciprocal Relations in Irreversible Processes. I, Phys. Rev. 37 (1931) 405–426, https://doi.org/10.1103/PhysRev.37.405.
[23] J.C. Maxwell, On the dynamical theory of gases, Philosophical Transactions of the Royal Society (1867) 49–88.
[24] J. Stefan, Über das Gleichgewicht und Bewegung, insbesondere die Diffusion von Gasgemengen, Sitzungsberichte der Akademie der Wissenschaften 1871 (1871) 63–124.
[25] J. Newman, D. Bennion, C.W. Tobias, Mass Transfer in Concentrated Binary Electrolytes, Ber Bunsenges Phys Chem 69 (1965) 608–612, https://doi.org/10.1002/bbpc.19650690712.
[26] A. Mistry, L.S. Grundy, D.M. Halat, J. Newman, N.P. Balsara, V. Srinivasan, Effect of Solvent Motion on Ion Transport in Electrolytes, J. Electrochem. Soc. 169 (2022) 40524, https://doi.org/10.1149/1945-7111/ac6329.
[27] M. Schammer, B. Horstmann, A. Latz, Theory of Transport in Highly Concentrated Electrolytes, J. Electrochem. Soc. 168 (2021) 26511, https://doi.org/10.1149/1945-7111/abdddf.
[28] S.T.P. Psaltis, T.W. Farrell, Comparing Charge Transport Predictions for a Ternary Electrolyte Using the Maxwell–Stefan and Nernst–Planck Equations, J. Electrochem. Soc. 158 (2011) A33, https://doi.org/10.1149/1.3509776.
[29] M. Lagnoni, C. Nicolella, A. Bertei, Comparison of Electrolyte Transport Modelling in Lithium-ion Batteries: Concentrated Solution Theory Vs Generalized Nernst-Planck Model, J. Electrochem. Soc. 169 (2022) 20570, https://doi.org/10.1149/1945-7111/ac51f4.
[30] J.T. Vardner, S.T. Russell, N.W. Brady, Y. Inaba, S.K. Kumar, A.C. West, Application of Concentrated Solution Theory to the Measurement of Salt Transference Numbers in Ion-Selective Membranes, J. Electrochem. Soc. 167 (2020) 20546, https://doi.org/10.1149/1945-7111/ab6c52.
[31] M. Vynnycky, K.I. Borg, On the application of concentrated solution theory to the forced convective flow of excess supporting electrolyte, Electrochim. Acta 55 (2010) 7109–7117, https://doi.org/10.1016/j.electacta.2010.06.070.
[32] T. León, J. López, R. Torres, J. Grau, L. Jofre, J.L. Cortina, Time-dependent 2-D model for transport of species analysis in electrodialysis: Concentration profiles and fluxes, Desalination. 565 (2023) 116819, https://doi.org/10.1016/j.desal.2023.116819.
[33] K.R. Kim, CFD Approach to Investigating Electrochemical Hydrodynamics and Mass Transport in a Copper Electrodeposition Process Using a Rotating Disk

Electrode, Int. J. Electrochem. Sci. (2021) 210239, https://doi.org/10.20964/2021.02.14.
[34] F.F. Rivera, L. Castañeda, P.E. Hidalgo, G. Orozco, Study of Hydrodynamics at AsahiTM prototype electrochemical flow reactor, using computational fluid dynamics and experimental characterization techniques, Electrochim. Acta 245 (2017) 107–117, https://doi.org/10.1016/j.electacta.2017.05.134.
[35] E.P. Rivero, M.R. Cruz-Díaz, F.J. Almazán-Ruiz, I. González, Modeling the effect of non-ideal flow pattern on tertiary current distribution in a filter-press-type electrochemical reactor for copper recovery, Chemical Engineering Research and Design 100 (2015) 422–433, https://doi.org/10.1016/j.cherd.2015.04.036.
[36] A. Van-Brunt, P.E. Farrell, C.W. Monroe, Structural electroneutrality in Onsager–Stefan–Maxwell transport with charged species, Electrochim. Acta 441 (2023) 141769, https://doi.org/10.1016/j.electacta.2022.141769.
[37] G. Litrico, C.B. Vieira, E. Askari, P. Proulx, Investigation of the Optimum Operative Conditions for a Parallel Plate Electrochemical Reactor, ECS. Trans. 75 (2017) 37–57, https://doi.org/10.1149/07537.0037ecst.
[38] J.W. Haverkort, H. Rajaei, Electro-osmotic flow and the limiting current in alkaline water electrolysis, Journal of Power Sources Advances 6 (2020) 100034, https://doi.org/10.1016/j.powera.2020.100034.
[39] R. Akolkar, Mathematical model of the dendritic growth during lithium electrodeposition, J. Power. Sources. 232 (2013) 23–28, https://doi.org/10.1016/j.jpowsour.2013.01.014.
[40] M. SCHMUCK, ANALYSIS OF THE NAVIER–STOKES–NERNST–PLANCK–POISSON SYSTEM, Math. Models Methods Appl. Sci. 19 (2009) 993–1014, https://doi.org/10.1142/S0218202509003693.
[41] Z. Song, X. Cao, H. Huang, Electroneutral models for dynamic Poisson-Nernst-Planck systems, Phys. Rev. e 97 (2018) 12411, https://doi.org/10.1103/PhysRevE.97.012411.
[42] J.J. Jasielec, R. Filipek, K. Szyszkiewicz, J. Fausek, M. Danielewski, A. Lewenstam, Computer simulations of electrodiffusion problems based on Nernst–Planck and Poisson equations, Comput. Mater. Sci. 63 (2012) 75–90, https://doi.org/10.1016/j.commatsci.2012.05.054.
[43] T. Sokalski, A. Lewenstam, Application of Nernst–Planck and Poisson equations for interpretation of liquid-junction and membrane potentials in real-time and space domains, Electrochem. commun. 3 (2001) 107–112, https://doi.org/10.1016/s1388-2481(01)00110-2.
[44] E.A. Guggenheim, Studies of Cells with Liquid-Liquid Junctions. II, J. Phys. Chem. 34 (1930) 1758–1766, https://doi.org/10.1021/j150314a005.
[45] J.A. Hogendoorn, A.J. van der Veen, J. van der Stegen, J. Kuipers, G.F. Versteeg, Application of the Maxwell–Stefan theory to the membrane electrolysis process, Comput. Chem. Eng. 25 (2001) 1251–1265, https://doi.org/10.1016/S0098-1354(01)00697-4.
[46] V.M. Volgin, A.D. Davydov, Mass-transfer problems in the electrochemical systems, Russ J Electrochem 48 (2012) 565–569, https://doi.org/10.1134/S1023193512060146.
[47] Y.S. Choi, K.Y. Chan, Exact solutions of transport in a binary electrolyte, Journal of Electroanalytical Chemistry 334 (1992) 13–23, https://doi.org/10.1016/0022-0728(92)80557-K.
[48] Y.K. Kwok, C.C.K. Wu, Fractional step algorithm for solving a multi-dimensional diffusion-migration equation, Numerical Methods Partial 11 (1995) 389–397, https://doi.org/10.1002/num.1690110407.
[49] V.M. Volgin, A.D. Davydov, Numerical Modeling of Steady-State Ion Transfer in Electrochemical Systems with Allowance for Migration, Russ J Electrochem 37 (2001) 1197–1205, https://doi.org/10.1023/A:1012771700852.
[50] M. Schalenbach, L. Keller, B. Janotta, A. Bauer, H. Tempel, H. Kungl, M. Bonnet, R. A. Eichel, The Effect of Ion Exchange Poisoning on the Ion Transport and Conduction in Polymer Electrolyte Membranes (PE, Universitätsbibliothek der RWTH Aachen, Aachen, 2022.
[51] G. Bauer, V. Gravemeier, W.A. Wall, A 3D finite element approach for the coupled numerical simulation of electrochemical systems and fluid flow, Numerical Meth Engineering 86 (2011) 1339–1359, https://doi.org/10.1002/nme.3107.
[52] A.V. Kovalenko, V.V. Nikonenko, N.O. Chubyr, M. Urtenov, Mathematical modeling of electrodialysis of a dilute solution with accounting for water dissociation-recombination reactions, Desalination. 550 (2023) 116398, https://doi.org/10.1016/j.desal.2023.116398.
[53] N. Jarvey, F. Henrique, A. Gupta, Ion Transport in an Electrochemical Cell: A Theoretical Framework to Couple Dynamics of Double Layers and Redox Reactions for Multicomponent Electrolyte Solutions, J. Electrochem. Soc. 169 (2022) 93506, https://doi.org/10.1149/1945-7111/ac908e.
[54] B.B. Owen, R.W. Gurry, The Electrolytic Conductivity of Zinc Sulfate and Copper Sulfate in Water at 25° 1, J. Am. Chem. Soc. 60 (1938) 3074–3078, https://doi.org/10.1021/ja01279a068.
[55] R.A. Noulty, D.G. Leaist, Diffusion in aqueous copper sulfate and copper sulfate-sulfuric acid solutions, J. Solution. Chem. 16 (1987) 813–825, https://doi.org/10.1007/BF00650751.
[56] M. Bešter-Rogač, Electrical Conductivity of Concentrated Aqueous Solutions of Divalent Metal Sulfates, Journal of Chemical & Engineering Data 53 (2008) 1355–1359, https://doi.org/10.1021/je8001255.
[57] L.A. Woolf, A.W. Hoveling, Mutual diffusion coefficients of aqueous copper(II) sulfate solutions at 25.deg, J. Phys. Chem. 74 (1970) 2406–2408, https://doi.org/10.1021/j100705a031.
[58] Thomas W. Chapman, The transport properties of concentrated electrolytic solutions: Ph.D. Thesis, 1967.
[59] M.S. Moats, J. Hiskey, D.W. Collins, The effect of copper, acid, and temperature on the diffusion coefficient of cupric ions in simulated electrorefining electrolytes, Hydrometallurgy 56 (2000) 255–268, https://doi.org/10.1016/S0304-386X(00)00070-0.
[60] W. Hittorf, Ueber die Wanderungen der Ionen während der Elektrolyse, Ann. Phys. 182 (1859) 337–411, https://doi.org/10.1002/andp.18591820302.
[61] B. Pillay, J. Newman, Modeling Diffusion and Migration in Dilute Electrochemical Systems Using the Quasi-Potential Transformation, J. Electrochem. Soc. 140 (1993) 414–420, https://doi.org/10.1149/1.2221060.
[62] S. Sarkar, W. Aquino, Electroneutrality and ionic interactions in the modeling of mass transport in dilute electrochemical systems, Electrochim. Acta 56 (2011) 8969–8978, https://doi.org/10.1016/j.electacta.2011.07.128.
[63] A. Katagiri, Calculation of steady-state distributions of concentrations and potential controlled by diffusion and migration of ions, J. Appl. Electrochem. 21 (1991) 487–495, https://doi.org/10.1007/BF01018600.
[64] S. Mafe, J. Pellicer, V.M. Aguilella, Ionic transport and space charge density in electrolytic solutions as described by Nernst-Planck and Poisson equations, J. Phys. Chem. 90 (1986) 6045–6050, https://doi.org/10.1021/j100280a117.
[65] S. Mafé, J.A. Manzanares, J. Pellicer, The charge separation process in non-homogeneous electrolyte solutions, J. Electroanal. Chem. Interfacial. Electrochem. 241 (1988) 57–77, https://doi.org/10.1016/0022-0728(88)85116-7.
[66] V.M. Aguilella, S. Mafé, J. Pellicer, On the nature of the diffusion potential derived from Nernst-Planck flux equations by using the electroneutrality assumption, Electrochim. Acta 32 (1987) 483–488, https://doi.org/10.1016/0013-4686(87)85018-1.